Pleiotropic effects of HIF-1 blockade on tumor radiosensitivity

Benjamin J. Moeller,[1] Matthew R. Dreher,[2] Zahid N. Rabbani,[3] Thies Schroeder,[3] Yiting Cao,[1] Chuan Y. Li,[3] and Mark W. Dewhirst[1,2,3,*]

[1]Department of Pathology
[2]Department of Biomedical Engineering
[3]Department of Radiation Oncology, Duke University Medical Center, Durham, North Carolina 27710
*Correspondence: dewhirst@radonc.duke.edu

Summary

We have previously shown that radiation increases HIF-1 activity in tumors, causing significant radioprotection of the tumor vasculature. The impact that HIF-1 activation has on overall tumor radiosensitivity, however, is unknown. We reveal here that HIF-1 plays an important role in determining tumor radioresponsiveness through regulating four distinct processes. By promoting ATP metabolism, proliferation, and p53 activation, HIF-1 has a radiosensitizing effect on tumors. Through stimulating endothelial cell survival, HIF-1 promotes tumor radioresistance. As a result, the net effect of HIF-1 blockade on tumor radioresponsiveness is highly dependent on treatment sequencing, with "radiation first" strategies being significantly more effective than the alternative. These data provide a strong rationale for pursuing sequence-specific combinations of HIF-1 blockade and conventional therapeutics.

Introduction

Radiation plays an important role in the treatment of cancer. Although modern technology has made it an effective tool, dose-limiting normal tissue toxicities and radioresistant tumors still lead to life-threatening radiation treatment failures. In order to improve its therapeutic ratio, there has been much interest in augmenting the effect of radiation on tumors by combining it with molecularly targeted tumor therapeutics (Camphausen and Tofilon, 2004). As this approach is beginning to show promise, there is a continued need for the discovery of novel critical molecular targets whose inhibition might enhance radiotherapeutic response.

Hypoxia-inducible factor-1 (HIF-1) is an excellent potential candidate for targeted inhibition to improve radiation outcome. It is a nuclear transcription factor whose activity is promoted by hypoxia (Wang and Semenza, 1993), oxidative stress (Chandel et al., 1998), and oncogenes (Laughner et al., 2001; Zundel et al., 2000); as such, it is commonly upregulated in tumors (Zhong et al., 1999). It influences tumor biology by regulating 60+ genes that contribute to crucial behaviors such as angiogenesis (Maxwell et al., 1997), cell death (Sowter et al., 2001), and metabolism (Firth et al., 1995; Semenza et al., 1994). The importance of HIF-1 is underscored by its association with poor disease-specific outcomes for multiple cancer types (Bos et al., 2003; Shibaji et al., 2003). It also plays a very important role in modulating treatment responsiveness. High tumor HIF-1 activity is an independent predictor of poor prognosis after radiotherapy (Aebersold et al., 2001; Koukourakis et al., 2002). For this reason, the interplay between radiotherapy and HIF-1 warrants detailed investigation.

We recently found that ionizing radiation significantly upregulates HIF-1 activity in tumors (Moeller et al., 2004). Radiation causes tumor oxygenation to increase, causing, in turn, both the accumulation of tumor-reactive oxygen/nitrogen species and the depolymerization of stress granules. These two events lead to increased expression of HIF-1 and its target downstream genes. As a result, the increased expression of HIF-1-regulated cytokines delivers survival signals to tumor endothelium, resulting in tumor radioresistance through vascular radioprotection.

This prior work strongly supports the claim that HIF-1 is a rational target for tumor radiosensitization. However, the complex roles of this protein require that caution be taken before moving this strategy forward. Many of the phenotypes regulated by HIF-1 activity are known modifiers of cellular radiosensitivity, including apoptotic potential (Rupnow and Knox, 1999), mitotic potential (Denekamp, 1986), and metabolic rate (Rojas and Denekamp, 1989). These pleiotropic effects make it diffi-

SIGNIFICANCE

Radiation is used in treating approximately 500,000 cancer patients in the United States annually. Consequently, many people could benefit from the development of new ways to make tumors respond better to radiation. We recently found that a crucial regulator of gene expression in tumors, HIF-1, is activated by radiation. We undertook the current study to determine how HIF-1 activation influences tumor radiosensitivity. Our results suggest that HIF-1 blockade may be a very effective means of overcoming tumor radioresistance. However, because HIF-1 influences radiosensitivity in many complex ways, the success of this strategy requires specific timing of its blockade relative to when radiotherapy is administered. This work may help optimize the use of HIF-1 inhibitors with conventional tumor therapies.

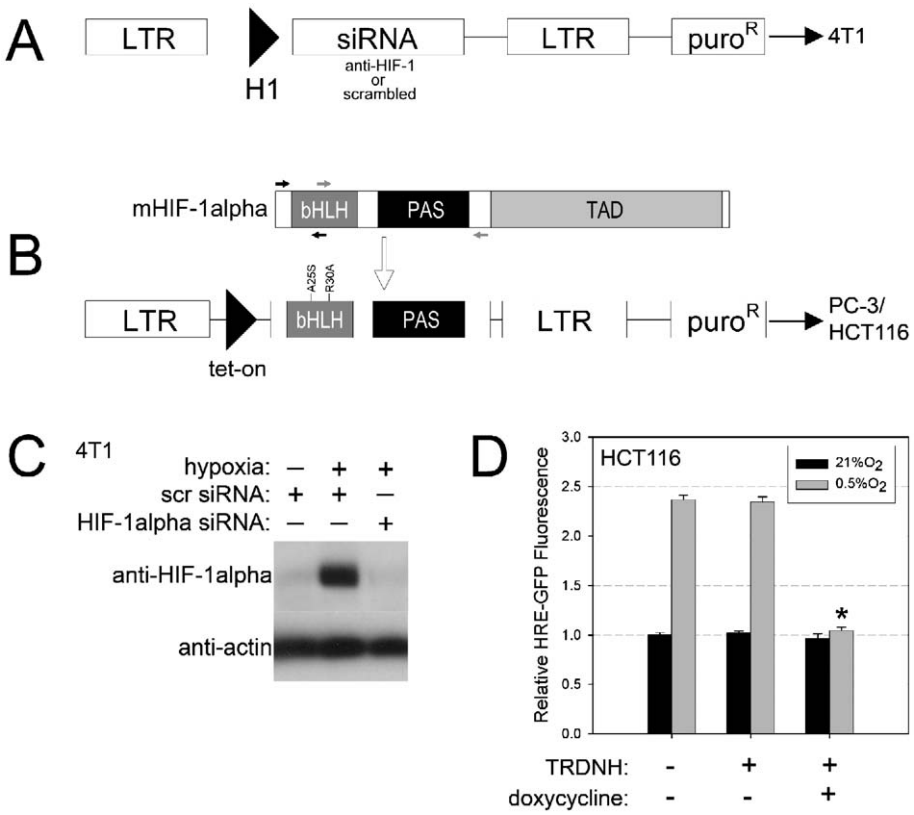

Figure 1. HIF-1 blockade model

A: Retroviral vectors were generated encoding *HIF-1α*-targeting or scrambled siRNA and transduced into 4T1 cells.

B: A dominant-negative HIF-1α mutant was created via site-directed PCR mutagenesis. Four primers (arrows) were used to amplify the N-terminal half of murine *HIF-1α* cDNA while mutating two residues in the DNA binding domain (A25S, R30A). This product was cloned into a retroviral vector and transduced into HCT116 and PC-3 cells.

C: 4T1 cells transduced with *HIF-1α*-targeting siRNA-expressing vectors demonstrated >90% HIF-1α protein knockdown by immunoblot.

D: HCT116 cells transduced with the tet-inducible dominant-negative HIF-1α (TRDNH) demonstrated complete repression of the hypoxia-stimulated increase in HRE-GFP fluorescence intensity upon exposure to doxycycline, with nonsignificant "leakiness" in the absence of doxycycline (*$p < 0.05$ versus 21% O_2). PC-3 cells demonstrated similar results (data not shown). Error bars represent the standard deviation of the mean.

cult to predict whether a HIF-1-inhibiting strategy would have an overall positive or negative impact on tumor radiosensitivity.

Therefore, we investigate here (1) how HIF-1 blockade influences tumor apoptosis, metabolism, proliferation, and angiogenesis, and (2) how each of these factors, in turn, affects radiosensitivity. The results of these studies are then used to rationally design and test strategies for the optimal timing of HIF-1 blockade relative to radiotherapy. This work may be vital to the clinical development of HIF-1 inhibitors for use with other treatment modalities.

Results

Establishing models of HIF-1 inhibition

We first sought to establish high-specificity molecular models of HIF-1 inhibition using RNA interference and directed protein mutagenesis. Retroviral vectors were designed to generate constitutive expression of *HIF-1α*-targeting or scrambled siRNA in transduced 4T1 cells (Figure 1A). Also, a dominant-negative mutant was created from *HIF-1α* cDNA using site-directed mutagenesis (Figure 1B). "Stitching" PCR reactions were run on *HIF-1α* cDNA to mutate the 25th and 30th residues, which had been previously identified as critical for DNA binding and downstream gene transcription (Michel et al., 2002). Further, the primers were designed to amplify the amino-terminal half of the protein only, eliminating from the product the oxygen-dependent degradation motifs of the carboxy-terminal half of the protein. This resulted in a HIF-1α mutant with oxygen-independent stability and an inability to upregulate downstream gene expression. The PCR product was cloned into a retroviral vector designed to generate tetracycline-inducible expression of the dominant-negative mutant in transduced HCT116 and PC-3 cells.

These models were both very effective at inhibiting HIF-1. The level of HIF-1α knockdown achieved by siRNA in 4T1 cells was greater than 90% (Figure 1C). In HCT116 and PC-3 cells, the tetracycline-responsive dominant-negative HIF-1α construct was negligibly active in the absence of doxycycline, yet was a strong HIF-1 inhibitor in its presence (Figure 1D). Interestingly, 4T1 cells responded less well to the dominant-negative construct as compared to the anti-HIF-1α siRNA, and the converse was true for HCT116 and PC-3 cells (data not shown). Therefore, we used siRNA exclusively for 4T1 cells, and our HIF-1α mutant exclusively for HCT116 and PC-3 cells in the experiments to follow.

HIF-1 potentiates radiation-induced apoptosis

One way HIF-1 might impact tumor radiosensitivity is through modulating apoptosis. HIF-1 has been shown to affect apoptosis in several ways. It stimulates upregulation of the proapoptotic BNIP3 (Guo et al., 2001) and can directly stabilize p53 (An et al., 1998). There are also data to suggest that HIF-1 can exert an antiapoptotic influence under certain conditions (Akakura et al., 2001). It is likely that the overall impact of HIF-1 on apoptosis is context dependent.

With these factors in mind, we first used the *p53*$^{+/+}$ HCT116 line to examine how HIF-1 affects radiation-induced apoptosis. HCT116 cells were irradiated with or without first being ex-

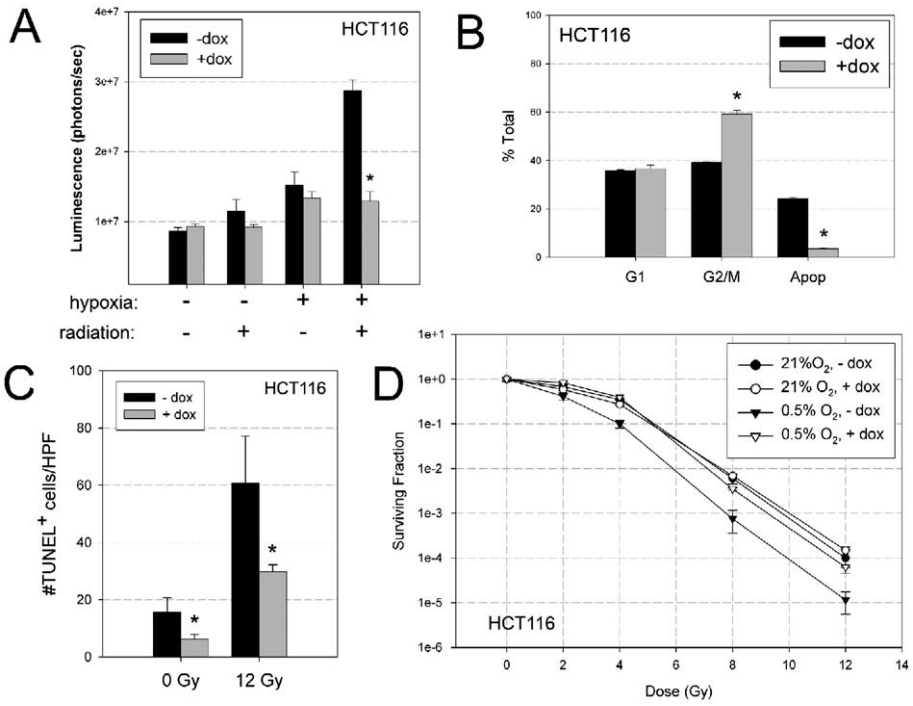

Figure 2. HIF-1 is required for hypoxic potentiation of radiation damage

A: Luminescent caspase 3/7 assay run on HCT116 cells 6 hr after treatment with 0 or 8 Gy of radiation. Cells were cultured for 24 hr under normoxia (21% O_2) or hypoxia (0.5% O_2) prior to irradiation. As with all experiments, hypoxic cells were reoxygenated for 10 min immediately before irradiation. Caspase activity was significantly enhanced after radiation for hypoxia-stimulated cells, through a HIF-1-dependent mechanism (*p < 0.05 versus −dox).

B: FACS analysis of DNA content in HCT116 cells 48 hr after receiving 8 Gy of radiation. Before irradiation, cells were stimulated by 24 hr of hypoxia and 10 min of reoxygenation. HIF-1 inhibition caused these cells to shift from apoptosis to G2/M arrest (*p < 0.05 versus −dox). S phase cells (data not shown) made up a very small percentage of the total population for both groups.

C: HCT116 tumors, with or without HIF-1 inhibition, were removed 48 hr after (sham) irradiation (3 × 4 Gy). Sections were labeled by TUNEL staining, and the results were quantified by counting the number of positive nuclei per high-powered field. HIF-1 inhibition significantly suppressed apoptosis (*p < 0.05 versus −dox). n = 5/group.

D: HCT116 cells were cultured for 24 hr under normoxia or hypoxia and in the presence or absence of doxycycline, reoxygenated briefly prior to irradiation, and assayed for clonogenicity 7 days after irradiation. Exposure to hypoxia before irradiation caused a significant left-shift in the survival curve (closed triangles; p < 0.05 versus 21% O_2 and −dox), and HIF-1 inhibition abrogated this response (open triangles).

Errors bars represent the standard deviation of the mean.

posed to a 24 hr period of hypoxia to activate HIF-1. Since hypoxia lowers the relative efficacy of radiation (Berry et al., 1970), hypoxic cells were reoxygenated 10 min prior to irradiation for this experiment as well as those to follow. This way, our results vary strictly as a function of differential hypoxia-induced gene and protein regulation, not as a function of the oxygen enhancement effect on radiation damage.

Caspase 3/7 activation and DNA fragmentation were used to analyze the effects of radiation on early (6 hr) and late (48 hr) apoptosis, respectively. There was a significant difference in the early apoptotic response to radiation between cells that had been cultured in normoxia and hypoxia before irradiation (hereafter referred to as "normoxic/irradiated" and "hypoxic/irradiated," respectively). Whereas normoxic/irradiated cells underwent only modest caspase activation at 6 hr, this response was markedly enhanced in the hypoxic/irradiated group (Figure 2A). This potentiation was completely absent in cells expressing the dominant-negative mutant, proving this to be a HIF-1-dependent effect. DNA content analysis of these cells 48 hr after irradiation demonstrated that a large fraction of the hypoxic/irradiated group proceeded from caspase activation to apoptosis (24.2% ± 0.5%), and that this fraction was markedly lower (3.6% ± 0.1%) in HIF-1-inhibited cells (Figure 2B). The decrease in the fraction of apoptotic cells in the HIF-1-inhibited group was balanced by an increase in the G2/M population (59.3% ± 1.4% +dox versus 39.3% ± 0.1% –dox), suggesting that the loss of HIF-1 shifts hypoxic/irradiated cells from apoptotic to G2-arrested fates.

The impact of HIF-1 inhibition on apoptosis was also examined for tumor cells grown in vivo (Figure 2C). TUNEL-positive nuclei were significantly less common in HIF-1-inhibited HCT116 tumors, both at baseline and 48 hr after irradiation.

Although these data indicate that HIF-1 inhibition protects hypoxic cells from radiation-induced apoptosis, this may not correlate with an effect on clonogenicity (Abend, 2003). From a therapeutic standpoint, if the excess G2-arrested population shown in Figure 2B does not eventually recover and demonstrate clonogenic capacity, the effect of HIF-1 blockade may be negligible. For this reason, clonogenic survival was determined for the HCT116 cells after radiation, with or without preincubation under hypoxia, and with or without stimulation by doxycycline (Figure 2D). Expressing the dominant-negative mutant had no impact on clonogenicity of aerobic cells following irradiation. In cells exposed to hypoxia before irradiation, on the other hand, clonogenic survival was significantly enhanced by HIF-1 blockade, with a 2-log-kill isoeffect dose-modifying factor (2L-DMF) of 1.22.

p53 is required for HIF-1-dependent apoptotic induction

Since it has been implicated previously in the link between HIF-1 and apoptosis, we next sought to determine whether p53 was required for the effects described above. HCT116 cells were cultured for 24 hr under normoxia or hypoxia, in the presence or absence of doxycycline stimulation, and briefly reoxygenated before irradiation. One hour after irradiation, nuclear extracts were prepared from these groups and run on a Western blot (Figure 3A). Radiation and hypoxia both led to increased p53 immunoreactivity in nuclear extracts, but combining the two stimuli did not further enhance this effect. Radi-

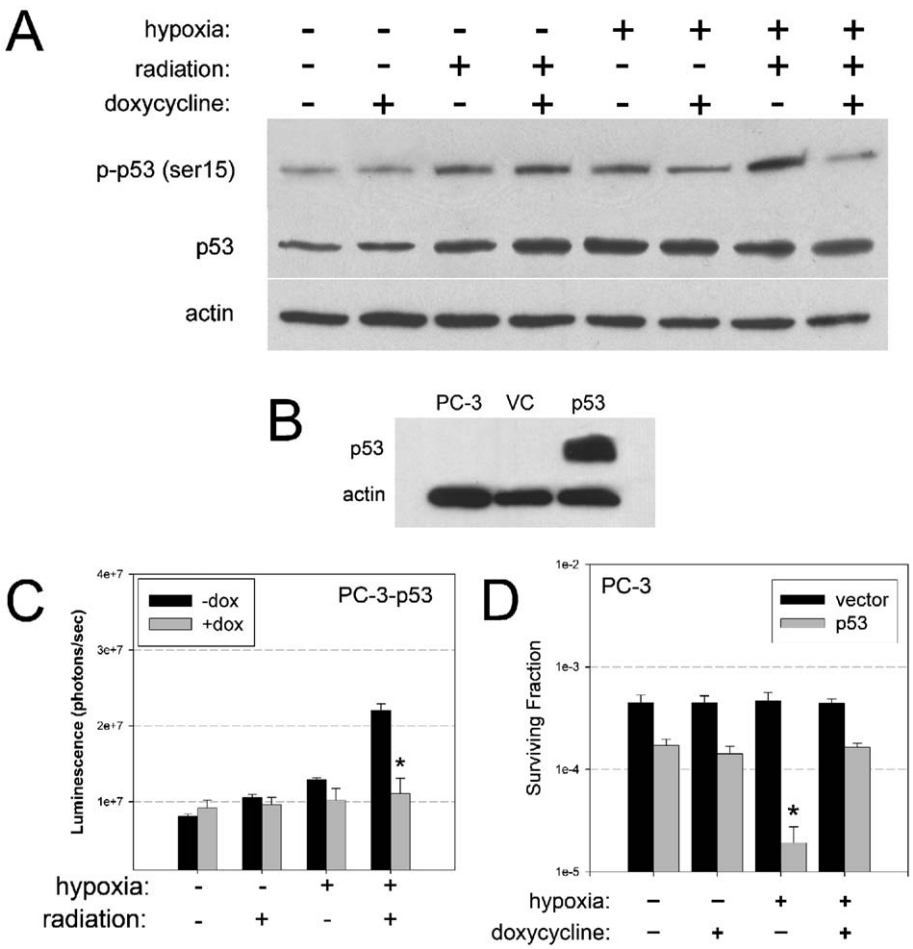

Figure 3. p53 is required for hypoxic potentiation of radiation damage

A: Immunoblots of nuclear extracts prepared from HCT116 cells 1 hr after radiation. Cells were exposed to normoxia (21% O_2) or hypoxia (0.5% O_2) for 24 hr, in the presence or absence of doxycycline, before irradiation (8 Gy).

B: Immunoblots of whole-cell extracts from PC-3 cells transduced with a *p53* expression vector (p53) or control vector (VC).

C: Caspase 3/7 assay run on *p53*-transduced PC-3 cells treated as in Figure 2A. Caspase activity was significantly enhanced in cells irradiated after hypoxic conditioning, in a HIF-1-dependent fashion (*$p < 0.05$ versus −dox). Error bars represent the standard deviation of the mean.

D: Clonogenicity of *p53*-transduced PC-3 cells treated as in Figure 2D prior to irradiation (10 Gy). Pretreatment with hypoxia significantly radiosensitized these cells ($p < 0.05$ versus 21% O_2 and −dox), through a HIF-1-dependent mechanism. Error bars represent the standard deviation of the mean.

ation and hypoxia also both led to increased phospho-p53 (serine 15) immunoreactivity, and combining the two stimuli lead to further p53 phosphorylation. Importantly, hypoxia/radiation-induced p53 phosphorylation was abrogated by HIF-1 inhibition. These data provide strong evidence, then, that HIF-1 is required for enhancement of radiation-induced p53 activation by hypoxia. They also suggest that p53 may be required for HIF-1-mediated potentiation of radiation-induced apoptosis by hypoxia.

To further investigate this latter hypothesis, we engineered a paired cell line in the PC-3 background distinguished only by p53 expression status. This was accomplished by transducing wild-type human *p53* cDNA (a generous gift from V. Seewaldt) into the *p53* null PC-3 cell line (Figure 3B). Taking advantage of the inducible HIF-1α mutant already established in this line, we were then able to study the effects of hypoxia on radiation-induced apoptosis in the presence or absence of both HIF-1 and p53 functionality. In native (*p53* null) PC-3 cells, exposure to hypoxia before radiation fails to augment subsequent caspase 3/7 activation, DNA fragmentation, or loss of clonogenic survival; accordingly, HIF-1 inhibition has no impact on these outcomes (see Figure S1 in the Supplemental Data available with this article online). For p53-expressing PC-3 cells, however, the response is quite different. As would be predicted, caspase 3/7 activity was increased across the board after *p53* reconstitution. However, caspase activity following hypoxia/irradiation was dramatically higher for the p53-expressing cells than it was for *p53* null PC-3 cells. Moreover, the caspase activity enhancement for this group was abrogated when HIF-1 was inhibited, as had been the case for the HCT116 cell line (Figure 3C). DNA content analysis after 48 hr showed that the *p53*-reconstituted PC-3 cells had a significant increase in the apoptotic population after hypoxia/irradiation (15.2% ± 0.4%), which was effectively blocked by HIF-1 inhibition (0.8% ± 0.4%). As was the case with the HCT116 line, the apoptotic cell population was shifted to G2 arrest in HIF-1-inhibited cells (data not shown). Finally, the impact of HIF-1 activity on the clonogenicity of hypoxic/irradiated cells was shown again here with *p53*-reconstituted PC-3 cells (Figure 3D). Once more, the clonogenicity of normoxic cells was not affected by HIF-1 blockade. The radiosensitivity of hypoxic, HIF-1-inhibited cells was similar to that of the normoxic cells. Hypoxic cells with intact HIF-1 function, on the other hand, were significantly less clonogenic following 10 Gy of radiation.

To summarize, HIF-1 promotes p53 phosphorylation at serine 15 in response to hypoxia and, more so, upon irradiation after hypoxic conditioning. As a consequence, HIF-1 and p53 are both required for hypoxic potentiation of radiation-induced caspase activation, apoptosis, and loss of clonogenicity.

HIF-1 maintains tumor energy metabolism

Recent work has provided strong evidence for the role of HIF-1 in regulating glucose metabolism and energy maintenance in tumors (Griffiths et al., 2002). Glucose levels and metabolic activity have been directly associated with tumor cell radiosensitivity (Heller and Raaphorst, 1994; Luk and Sutherland, 1987). Therefore, we sought to determine how HIF-1 inhibition would alter energy metabolism in tumors, and how this effect might influence overall radiosensitivity.

We first examined how HIF-1 inhibition influences glucose consumption in our models. 4T1 and HCT116 cells were exposed to 24 hr of normoxia or hypoxia, with or without HIF-1 inhibition, and were subsequently assayed for glucose consumption rates (Figure 4A). There was an enhancement of glucose consumption after exposure to hypoxia, and this effect was abrogated by HIF-1 blockade for both cell lines. We hypothesized that this impaired glucose utilization would lead to decreased ATP production in HIF-1-inhibited cells. To test this hypothesis, 4T1 and HCT116 cells were stressed by hypoxia for 24 hr, with or without glucose deprivation, with or without HIF-1 inhibition, and then assayed for total cellular ATP levels (Figure 4B). Neither hypoxia nor glucose deprivation alone was sufficient to deplete cellular ATP, whether the cells were HIF-1 inhibited or not (data not shown). When the two stressors were combined, however, ATP levels fell for both groups. Consistent with their impaired ability to consume glucose, the HIF-1-inhibited cells experienced a significantly greater reduction in ATP stores after the combined stress.

Next, 4T1 and HCT116 tumors were grown in mice to determine whether HIF-1 inhibition would influence ATP levels in vivo (Figure 4C). Bioluminescence imaging was used to quantify ATP concentrations in frozen tissue sections (Schwickert et al., 1996). HIF-1 blockade caused a 5-fold reduction in overall ATP levels for 4T1 tumors, and a 2-fold reduction for HCT116 tumors. Spatially, the loss of ATP was most significant near the center of HIF-1-inhibited tumors, with levels at the periphery being similar to that found in wild-type tumors. Similarly, HIF-1 blockade was also found to increase the area of central necrosis for both tumor types studied. The diameter of the viable rim of tumor identified by H&E staining was significantly smaller in HIF-1-inhibited tumors (4T1, 0.92 ± 0.48 mm; HCT116, 1.32 ± 0.63 mm) as compared to their controls (4T1, 4.94 ± 1.04 mm; HCT116, 3.29 ± 0.61 mm; $p < 0.05$; n = 5/group).

The above data indicate that HIF-1 inhibition impairs tumor energy metabolism, leading to a reduction in ATP levels and cellular viability. As reduced metabolic rates have been linked with radioresistance, we next examined whether inhibiting HIF-1 in nutrient-depleted cells would influence clonogenic survival after irradiation. Wild-type PC-3 cells were chosen for this experiment because hypoxia does not affect their clonogenicity after irradiation (Figure S1); therefore, oxygenation could be eliminated as a variable in the following experiment. PC-3 cells were cultured for 24 hr under hypoxia, in high or low glucose concentrations, with or without stimulation by doxycycline (Figure 4D). As before, the cells were briefly reoxygenated prior to irradiation. HIF-1 blockade failed to affect clonogenic survival in cells exposed to high glucose concentrations prior to irradiation. For cells cultured in low-glucose conditions, however, survival curves were significantly right shifted. Low glucose alone induced modest radioresistance in the PC-3 cells (2L-DMF = 1.14). Combining low glucose with HIF-1 blockade resulted in cells becoming significantly more radioresistant (2L-DMF = 1.49), consistent with the lowered energy state of these cells. We also compared survival curves for HCT116 cells exposed to hypoxia and doxycycline, with or without glucose deprivation (Figure S2). Low glucose concentrations induced radioresistance in these cells to a degree similar to that seen for PC-3 cells (2L-DMF = 1.31).

In summary, HIF-1 maintains glucose metabolism and ATP production in tumor cells, most prominently in the center of tumors, sustaining bioenergetics at a level required for high cellular sensitivity to radiation.

HIF-1 proliferation effects vary with microenvironment

It has been reported that HIF-1 is required for cell cycle arrest in response to hypoxia (Goda et al., 2003). Since cell cycle phase also influences radiosensitivity, we next sought to investigate whether HIF-1 inhibition might impact tumor radioresponsiveness through its effects on proliferation rate.

4T1 and PC-3 cells were cultured for 24 hr in hypoxic or normoxic conditions, with high or low glucose concentrations in the media. MTT assays showed that HIF-1-inhibited cells were more viable than controls after hypoxia alone, but less so after combined hypoxia and glucose deprivation (Figure 5A). Analysis of DNA content revealed that cell cycle arrest was at least in part responsible for these effects (Figure 5B). HIF-1 inhibition attenuated G1 blockade following hypoxia alone, consistent with its role in promoting hypoxic growth arrest. In contrast, the loss of HIF-1 promoted G1 arrest in response to combined oxygen and glucose deprivation.

To determine whether these results are relevant to the microenvironment encountered by tumors in vivo, patterns of cellular proliferation were analyzed in tumor sections using Ki-67 immunohistochemistry. There appeared to be qualitative differences between the groups in how proliferation indices varied with the distance from perfused vasculature (Figure 5C). Quantitative analysis of these data revealed that there was, indeed, distinct variation in the spatial patterns of proliferation between the wild-type and HIF-1-inhibited groups (Figure 5D). For both groups, proliferation indices fell off significantly as distance from the vasculature increased ($p < 0.05$), as expected. There was no significant effect of HIF-1 inhibition on the global proliferation indices for the groups ($p > 0.05$). However, there was a highly significant interaction between group and distance ($p < 0.001$). HIF-1 knockdown tumors were more proliferative in tissues near vasculature ($\leq$240 μm), whereas wild-type tumors were more proliferative in tissues far from vasculature ($\geq$240 μm). To control for potential differences in nuclear density between the groups, a similar analysis was run on sections counterstained for total nuclei. In general, nuclear densities decreased with distance from perfused vasculature for both groups, but there was no significant difference in nuclear density between the groups at any given distance ($p > 0.05$; data not shown).

We next examined whether HIF-1 influences radiosensitivity through regulating cellular proliferation rates. Wild-type PC-3 cells were again used here, as hypoxia does not affect their clonogenicity after radiation, eliminating oxygenation as an experimental variable. PC-3 cells were cultured under hypoxic conditions for 24 hr, with or without doxycycline stimulation, and with or without aphidicolin-induced cell cycle synchronization (Figure 5E). Next, the cells were briefly reoxygenated and

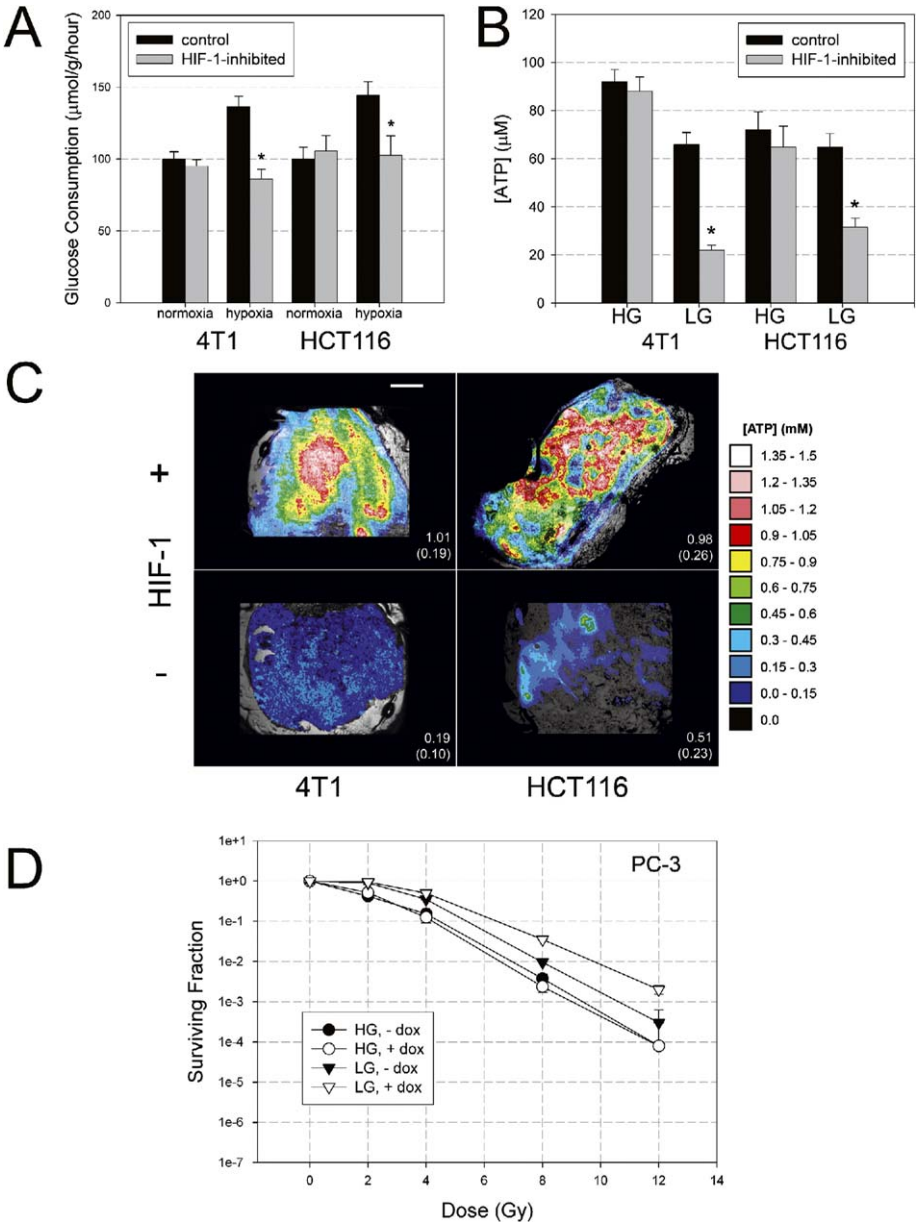

Figure 4. HIF-1 maintains tumor bioenergetics

A: Glucose consumption rates rise in 4T1 and HCT116 cells exposed to hypoxia (0.5% O_2) for 24 hr, and HIF-1 blockade completely inhibits this response (*p < 0.05 versus control). Error bars represent the standard deviation of the mean.

B: Whole-cell ATP levels in 4T1 and HCT116 exposed to a combination of low oxygen (0.5% O_2) and either high glucose (HG; 5 g/l) or low glucose (LG; 0.1 g/l) concentrations for 24 hr, with or without HIF-1 inhibition. ATP levels fall for each line in low-glucose conditions, but the effect is significantly more pronounced when HIF-1 is inhibited (*p < 0.05 versus control). Error bars represent the standard deviation of the mean.

C: Ex vivo ATP bioluminescence. ATP is significantly depleted in 4T1 and HCT116 tumors in response to HIF-1 blockade (p < 0.05). Representative images are shown, along with mean ATP concentrations (mM) displayed for each group, with standard deviations in parentheses. Scale bar, 500 μm. n = 5/group.

D: PC-3 cells were cultured for 24 hr under hypoxia, with high glucose (HG; 5 g/l)- or low glucose (LG; 0.1 g/l)-containing media, with or without doxycycline stimulation, and briefly reoxygenated prior to irradiation. Low glucose concentrations caused a significant right-shift in the survival curve (closed triangles; p < 0.05 versus HG and −dox), and HIF-1 inhibition further enhanced this effect (open triangles; p < 0.05 versus LG and −dox). Error bars represent the standard deviation of the mean.

then immediately irradiated. Aphidicolin, which causes G1/S cell cycle arrest, resulted in a slight right-shift in the survival curve for hypoxic cells (2L-DMF = 1.14), likely through arresting those cells which had escaped HIF-1-mediated cell cycle blockade. It caused a significantly greater shift toward radioresistance when applied to HIF-1-inhibited, hypoxic cells (2L-DMF = 1.31), wherein a larger fraction of cells had escaped G1 blockade secondary to HIF-1 dysfunction. Similar results were seen for HCT116 cells (Figure S3). These data suggest that HIF-1 normally acts to lower radiosensitivity in hypoxic cells by promoting cell cycle arrest. However, it also normally functions to sustain mitotic rates for cells starved of both glucose and oxygen, likely leading to relative radiosensitization of these cells. Therefore, the overall impact of HIF-1 activity on tumor radiosensitivity, due to its effects on proliferation, is likely dependent on the microenvironment.

HIF-1 promotes vessel radioresistance

HIF-1-inhibiting compounds, delivered after radiation, lead to significant destruction of tumor vasculature and prolonged time to tumor regrowth after therapy (Moeller et al., 2004). Were the sequence or timing of therapeutic delivery altered, however, it is unknown whether this approach would remain effective. It is possible, for example, that preradiation HIF-1 blockade might have antiangiogenic effects on tumors (Stoeltzing et al., 2004). This could, conceivably, compromise radiotherapy by decreasing tumor oxygenation—an effect previously described for another antiangiogenic therapy (Murata et al., 1997). Therefore, we next sought to investigate how HIF-1 blockade influenced tumor vascularity in our models, and whether the timing of HIF-1 inhibition would affect its overall impact on tumor vessel radiosensitivity.

To begin, we first examined how HIF-1 blockade affects early

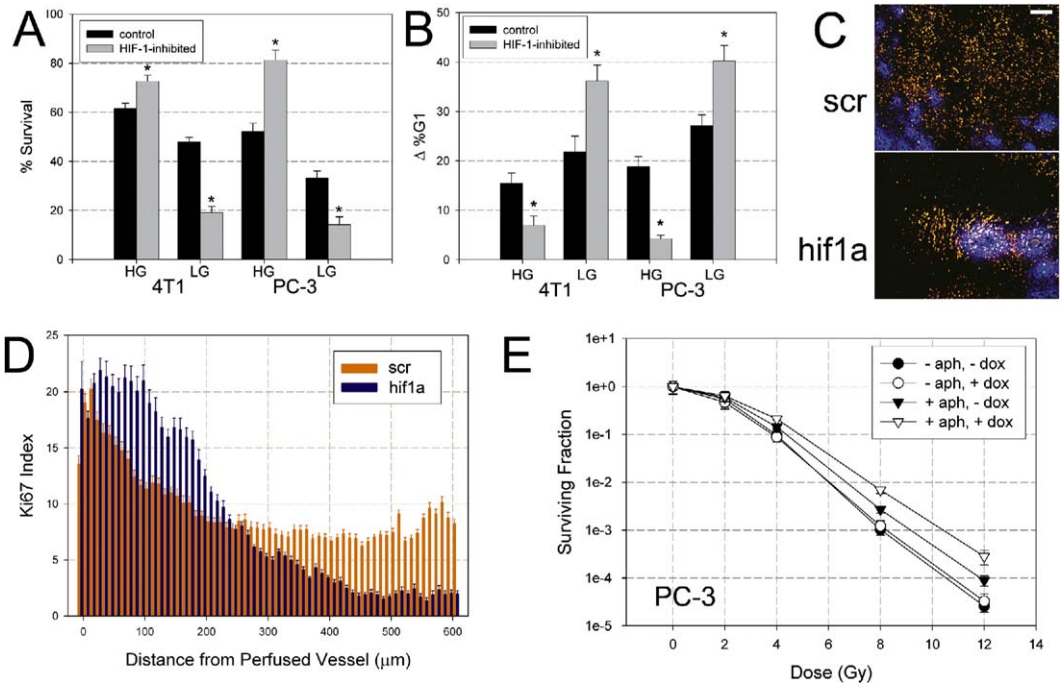

Figure 5. HIF-1 maintains proliferative capacity

A: Viability of 4T1 and PC-3 cells exposed to 24 hr of hypoxia (0.5% O_2) and high or low glucose (5 or 0.1 g/l) concentrations, as determined by MTT assay. HIF-1-inhibited cells fare significantly better under hypoxia alone, but significantly worse under hypoxia and low glucose (*$p < 0.05$ versus control). Results are normalized to the viability of cells at normoxia, in high-glucose media, without HIF-1 blockade.

B: Cell cycle analysis of 4T1 and PC-3 cells exposed to nutrient deprivation, as in **A**. Results are expressed as the change in size of the G1 population as compared to normoxic, high-glucose controls. HIF-1 inhibition attenuates G1 arrest after hypoxia but enhances it after hypoxia and glucose deprivation (*$p < 0.05$).

C: 4T1 tumors grown in vivo demonstrate varying spatial patterns of proliferative indices depending on HIF-1 activity. Representative fields are shown. Blue, IV-injected perfusion marker (Hoechst 33342); red, proliferation marker (Ki-67). Scale bar, 100 μm. Similar results were obtained for PC-3 tumors (data not shown).

D: The Ki-67 index (percentage Ki-67$^+$ area) was quantified for 4T1 tumors in 10 μm bins extending from perfused vessels, out to a maximum of 605 μm. n = 5/group.

E: Clonogenic assay for PC-3 cells cultured for 24 hr under hypoxia, with or without doxycycline, with or without aphidicolin (5 μg/ml), and irradiated following a brief period of reoxygenation. Cell cycle synchronization with aphidicolin caused a significant right-shift in the survival curves (open symbols; $p < 0.05$ versus −aph), more pronounced when combined with HIF-1 blockade ($p < 0.05$ versus −dox + aph).

Error bars represent the standard deviation of the mean.

tumor angiogenesis. We elected against using our dominant-negative model for this study, as we were concerned that transient HIF-1 activation, occurring before expression of the mutant could be induced in vivo, could have dramatic effects on angiogenesis. Therefore, we used our siRNA model for this study, measuring angiogenesis in 4T1 tumors by following their vascularity over time using dorsal skinfold window chambers. Since HIF-1 blockade had no effect on overall 4T1 tumor growth rate (data not shown), we could compare vascularity between groups over time without adjusting for tumor volume. There was a delay in initial tumor vascularization in the HIF-1-inhibited tumor group, most pronounced at day 10 following tumor cell inoculation (Figure 6A). After that point, however, there were no significant differences in vascular density between the two treatment groups. Next, immunohistochemistry was used to determine whether this parity in angiogenesis held for larger tumors (volume, 1000 mm^3; n = 5/group). Vascular density, vessel maturity, and tumor oxygenation were all similar for both control and knockdown tumors (see the Supplemental Data).

Though it did not appear to alter baseline tumor vessel anatomy or physiology, our prior work suggests that HIF-1 inhibition dramatically increases tumor vessel radiosensitivity. Therefore, we next sought to determine (1) whether our biological, high-specificity models of HIF-1 inhibition also radiosensitized tumor vasculature, and (2) whether the timing of HIF-1 inhibition with radiotherapy would impact this result. We used 4T1, HCT116, and PC-3 tumors, grown in the dorsal skinfold window chamber, to monitor changes in tumor vascularity over time following HIF-1 blockade and radiotherapy. 4T1 knockdown tumors underwent significant vascular regression following irradiation, whereas control tumor vessel density trended higher (Figure 6B). Next, pre- and postradiation doxycycline treatments were tested on HCT116 and PC-3 window chamber tumors to determine whether these sequences would cause differential vascular radiosensitization. Each combination induced significant tumor devascularization as compared to radiation alone, with neither sequence being more effective at doing so than the other (Figure 6C). Therefore, HIF-1 blockade is

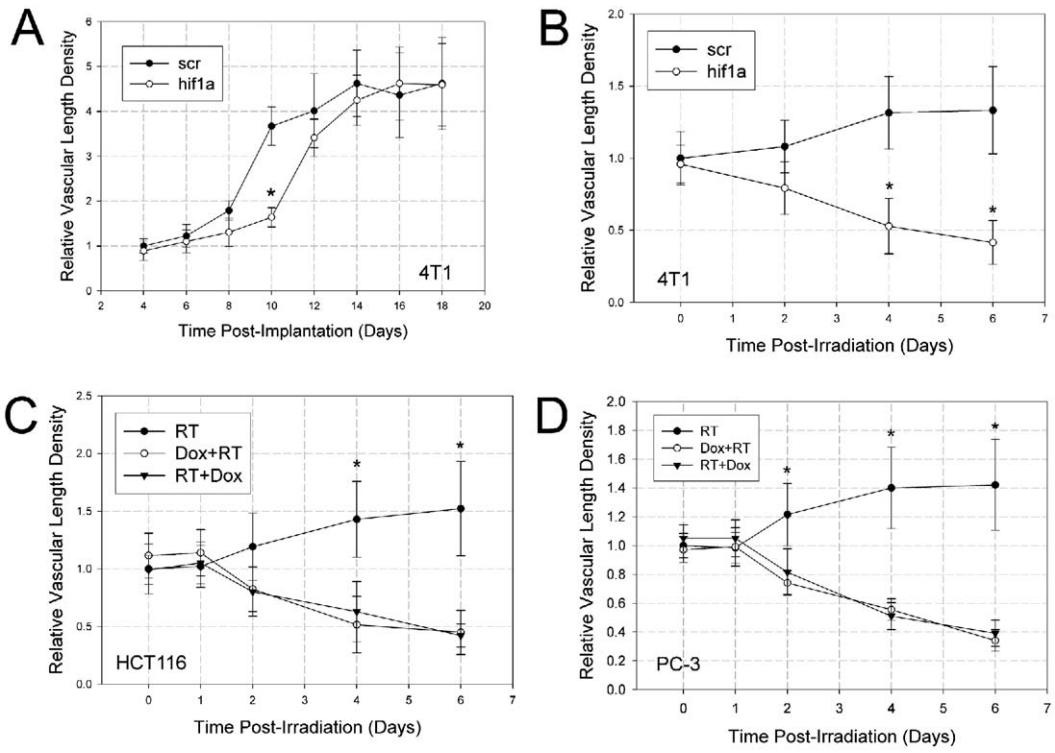

Figure 6. HIF-1 protects tumor vasculature

A: Serial monitoring of vascular length density in 4T1 window chamber tumors. Angiogenesis was slightly delayed in HIF-1 knockdown tumors, but tumor vascularity was significantly different from controls only on day 10 (*$p < 0.05$ versus scrambled siRNA control). n = 5/group.

B: Vascular length density in 4T1 window chamber tumors following three 3 Gy fractions of radiation. Knockdown tumors underwent devascularization beginning 48 hr after irradiation (*$p < 0.05$). n = 5/group.

C and D: Vascular length density in HCT116 (**C**) and PC-3 (**D**) window chamber tumors following irradiation (3 × 3 Gy). Doxycycline exposure began 1 week prior to radiation (Dox + RT), or immediately after radiation (RT + Dox). Vascular regression occurred to similar degrees for both groups treated with radiation and doxycycline, regardless of sequencing (*$p < 0.05$ versus Dox + RT and RT + Dox). Doxycycline alone did not affect vascular density (data not shown). n = 5/group.

Error bars represent the standard deviation of the mean.

an effective means of enhancing radiation damage to tumor vasculature, irrespective of treatment sequencing.

HIF-1 blockade is maximally effective following radiation

Results from the above experiments suggest that HIF-1 influences tumor cell radiosensitivity through multiple mechanisms. By promoting apoptosis, metabolism, and proliferation of nutrient-starved cells, HIF-1 *enhances* tumor radiosensitivity. In contrast, HIF-1 also dramatically *decreases* tumor radiosensitivity through cytokine-mediated protection of tumor vasculature. Importantly, the time course over which these opposing mechanisms occur is likely distinct, raising the possibility that the proper timing of HIF-1 blockade could optimize its effects on radiotherapy. Specifically, the effects of HIF-1 inhibition on apoptosis, metabolism, and proliferation would be expected to influence the immediate response of tumors to ionizing damage; therefore, these mechanisms may not significantly influence treatment outcome unless modified before radiation is delivered. Consistent with this hypothesis, we found that postradiation HIF-1 blockade failed to modify tumor cell clonogenicity in situations where preradiation HIF-1 inhibition had succeeded in doing so (Figure S4). The vascular effects of HIF-1 blockade, on the other hand, have been shown here to cause radiosensitization regardless of sequencing with radiation (Figure 6); therefore, this mechanism could significantly influence treatment outcome whether modified before or after radiotherapy. Based on this reasoning, it was hypothesized that postradiation HIF-1 blockade would have significantly greater antitumor effects than would preradiation HIF-1 inhibition.

To test this hypothesis, HCT116 and PC-3 tumors were randomized to the treatment groups outlined in Figure 7A, and the corresponding growth delay data are displayed in Figures 7B and 7C. Average tumor volumes among the various treatment groups for each tumor line were not significantly different at the times of randomization (1 week postimplantation) or irradiation (2 weeks postimplantation). Subsequent growth rates were not affected by HIF-1 inhibition alone. Combining HIF-1 blockade with radiation, however, significantly enhanced tumor growth delay. For HCT116 tumors, the efficacy of this approach was highly dependent on sequencing. Preradiation HIF-1 blockade extended the time to reach 5× initial treatment volume by approximately 3 days ($p < 0.05$ versus radiotherapy [RT] alone). Postradiation HIF-1 inhibition extended the same interval by 15 days ($p < 0.001$ versus RT alone). By this metric, the "radiation

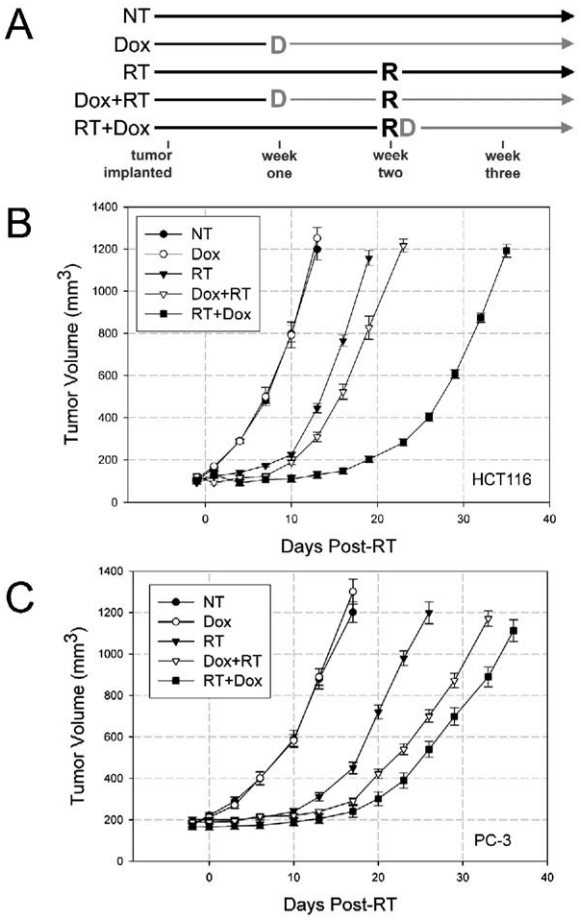

Figure 7. Sequencing determines effect of HIF-1 inhibition on radiation

A: A treatment timeline is shown for each group, indicating the times of tumor implantation, initial doxycycline exposure (D), and irradiation (R), along with the length of doxycycline exposure (gray arrow). Radiation was given in three 4 Gy fractions spaced by 12 hr each. Doxycycline treatment began in group 5 immediately following the last fraction of radiation. Tumor growth delay data are shown for HCT116 (**B**) and PC-3 (**C**) tumors. Tumor regrowth after treatment was significantly delayed for all irradiated groups ($p < 0.05$ versus NT). Preradiation doxycycline treatment caused a significantly prolonged growth delay ($p < 0.05$ versus RT) for both tumor types. Postradiation doxycycline treatment caused a marked enhancement in growth delay, significantly greater than that for both of the other irradiated groups ($p < 0.05$). The difference in efficacy between the two sequencing schema was much more pronounced for HCT116 tumors as compared to PC-3 tumors. n = 8/group. Error bars represent the standard deviation of the mean.

first" strategy extended tumor growth delay for HCT116 tumors five times further than did the alternative sequencing. For PC-3 tumors, the difference in efficacy between the two sequencing strategies was much less pronounced. Preradiation HIF-1 blockade caused significant growth delay ($p < 0.05$ versus RT alone), extending the time to reach 5× initial treatment volume by approximately 8 days. Postradiation HIF-1 inhibition also significantly prolonged the growth delay ($p < 0.05$ versus RT alone) and extended the 5× regrowth time by approximately 10 days. Therefore, the efficacy of combined radiotherapy and HIF-1 inhibition is dependent on the sequencing of treatments, but the magnitude of the sequencing effect may vary from tumor to tumor.

Discussion

The idea that HIF-1 may be a good target for cancer therapy is not a new one (Giaccia et al., 2003; Semenza, 2003). HIF-1 is active in virtually all tumors, and it plays key roles in promoting malignant behavior. Moreover, some preclinical studies on xenograft tumors have shown that HIF-1 inhibition slows tumor growth (Kung et al., 2000), while its activation accelerates growth (Ravi et al., 2000). Though these data establish the rationale for using HIF-1 blockade as a single-modality cancer therapy, work done previously by our group suggests that HIF-1 blockade will work best when combined with other treatments such as radiotherapy.

However, as discussed above, HIF-1 may also serve to radiosensitize tumors through various mechanisms. Indeed, we have demonstrated here that HIF-1 can enhance tumor radiosensitivity through increasing apoptotic potential, proliferation rates, and ATP metabolism. Because the importance of these effects varies with the tumor microenvironment and target cell type, the impact of HIF-1 inhibition is also likely to differ depending on location within the tumor (Table 1). HIF-1 blockade has pronounced radiosensitizing effects on tumor vasculature, seemingly irrespective of vessel location. The impact of HIF-1 inhibition on radiosensitivity of tumor cells, on the other hand, probably depends strongly on the local physiological microenvironment. For well-oxygenated tumor cells, HIF-1 is unlikely to be active, and its inhibition is probably not consequential. For hypoxic cells with sufficient access to glycolytic energy stores, HIF-1 inhibition will increase proliferation rates by abrogating G1 blockade mechanisms while decreasing apoptotic potential by suppressing p53 activation—the balance of these two effects would likely minimize the overall impact on radiosensitivity for these cells. For tumor cells low on oxygen *and* nutrients, called "distal" cells here, HIF-1 inhibition would likely lead to significant radioresistance.

Were these two compartments—vasculature and distal tumor cells—equally affected by HIF-1 inhibition, the ultimate impact on radiosensitivity would depend on which is the more important determinant of radiation outcome. A strong case has recently been made for the importance of tumor vasculature in determining radiosensitivity (Garcia-Barros et al., 2003). An equally compelling argument could be made for the importance of distal tumor cells. Bordering on necrosis, these cells are initially protected from radiation damage by their microenvironment. As tumors reoxygenate and reperfuse during fractionated radiotherapy, they can overcome their prior growth restrictions and contribute to treatment failure. Therefore, it is conceivable that both of these compartments, with radiosensitivities highly dependent on HIF-1 activity, could contribute strongly to overall tumor radioresponsiveness.

If one hopes to optimize the combination of HIF-1-inhibiting and cytotoxic therapies, then, the strategy used should aim to maximize the effects of HIF-1 blockade on the vasculature while minimizing effects on the distal tumor cells. This could be achieved either through spatial or temporal selectivity of HIF-1 blockade. Since tumor vasculature is most influenced by cytokine secretion from nearby ("proximal") tumor cells, spatial targeting of HIF-1 inhibition to the vasculature could be accom-

Table 1. Summary of results

Compartment	Apoptosis		Metabolism		Proliferation		Radiosensitivity
Vasculature	↑	+	↔	+	↔	=	↑
Proximal tumor	↓	+	↔	+	↑	=	↔
Distal tumor	↓	+	↓	+	↓	=	↓

HIF-1 inhibition either increases (↑), decreases (↓), or has no effect on (↔) tumor and endothelial cell apoptosis, metabolism, and proliferation; the sum total of these effects determines how it influences radiosensitivity. "Proximal tumor" refers to tumor cells near perfused vasculature that are hypoxic but supplied with nutrients; "distal tumor" refers to tumor cells far from perfused vasculature that are both hypoxic and nutrient depleted.

plished by delivering the inhibitory agent via macromolecular carriers that penetrate only as far as these cells are located. An alternative, somewhat simpler approach would be to target the effects of HIF-1 blockade to tumor vasculature through specific timing of therapeutic delivery, as was done here. The window of opportunity for radiosensitizing tumor vessels with HIF-1 inhibition was large, since the sequencing of treatments was irrelevant. The therapeutic window for changing tumor cell radiosensitivity with HIF-1 blockade is narrower, as demonstrated above. Since HIF-1 mainly modulates processes that influence the immediate response to ionizing radiation damage in tumor cells, HIF-1 must be inhibited prior to irradiation to have an effect in this compartment. Therefore, "radiation first" sequencing maximizes the efficacy of combining HIF-1 blockade with cytotoxic therapy by preferentially exploiting the antivascular component of this strategy.

Due to promising preclinical trials, there is much interest in developing new targeted therapy strategies for radiosensitizing tumor vasculature. We feel that HIF-1 should be a leading candidate among those proposed so far. Because it targets signaling pathways that promote vascular radioresistance in tumors, but not in normal tissues, HIF-1 blockade is a tumor-specific approach to this problem. By targeting multiple nonoverlapping vascular-protecting pathways at their upstream source, HIF-1 blockade is also a potent multifaceted approach to this problem. Moreover, the data presented here may underestimate the efficacy of this approach. Our model studied the effects of HIF-1 inhibition on tumor cells only, but its effects on stromal cells may be highly significant as well. It has recently been reported that HIF-1 activity is important within tumor endothelial cells themselves, wherein it serves to fuel an autocrine VEGF loop that maintains angiogenesis and vascularity (Tang et al., 2004). Since VEGF is a key promoter of endothelial radioresistance (Gorski et al., 1999), HIF-1 inhibition within tumor endothelial cells may increase overall tumor radiosensitivity beyond the levels seen here. Such a mechanism might counterbalance the protective effects of HIF-1 blockade for p53-expressing tumors, rendering the overall effect beneficial irrespective of the tumor cell radioprotection. This possibility certainly warrants further investigation.

Further underscoring the importance of coupling HIF-1 inhibition with radiation, our studies suggest that HIF-1 blockade may be an ineffective single-modality therapy. Several prior studies have reported tumor growth inhibition after HIF-1 blockade. However, many of these experiments used fibroblasts or stem cells derived from *HIF-1α* knockout mice instead of established tumor lines (Carmeliet et al., 1998; Ryan et al., 1998). HIF-1α mutant proteins have been used in the past to successfully reduce tumor growth rates (Kung et al., 2000), but to our knowledge, they have never before been used solely in already-established tumors as was done here. Since our approach seems more clinically relevant, we think it deserves careful consideration. In contrast, our model of constitutive HIF-1 blockade also failed to show tumor growth restriction. To our knowledge, no prior studies have used siRNA to inhibit HIF-1α activity in vivo—the discrepancy here may, therefore, be methodological. Future work will need to be done to clarify whether HIF-1 inhibition by itself is an effective anticancer tool.

This work may have important implications for the way in which HIF-1 inhibitors are used in the clinic. Our data suggest that HIF-1 blockade will be suboptimally effective if used prior to cytotoxic therapy. Although this sequencing may be a suitable approach for other antiangiogenic agents (Winkler et al., 2004), HIF-1 inhibitors might impede therapy if used this way. As an alternative, we propose that HIF-1 blockade should be used concurrently with chemotherapy and/or radiotherapy. One way to do so would be to administer HIF-1 blockade throughout the course of chemotherapy/radiotherapy, thereby maximally sensitizing the tumor vasculature. Alternatively, one could inhibit HIF-1 during breaks from treatment (e.g., over the weekend for fractionated radiotherapy or between cycles of chemotherapy), thereby minimizing the potential for interfering with their cytotoxicity.

It is also important to note that patient selection may play an eventual role in maximizing the potency of HIF-1 blockade. The mechanisms of radiation-induced HIF-1 activation are dependent on the presence of tumor hypoxia before treatment (Moeller et al., 2004). Therefore, methods of identifying tumors with high hypoxic fractions could be useful in selecting patients who will benefit from HIF-1 blockade during chemo/radiotherapy. Similarly, tumors found to have high HIF-1α expression levels may respond best to this type of treatment. There is already a large body of work demonstrating that HIF-1α expression correlates with poor clinical outcome (Semenza, 2002). If this at-risk population could be identified and offered HIF-1 blockade as adjunctive therapy, they might benefit greatly. It was also shown here that *p53* status is a major determinant of how HIF-1 affects tumor radiosensitivity. As a result, it may also be beneficial to use HIF-1 inhibition preferentially for tumors with documented *p53* mutations, as they will be less sensitive to its radioresistance-inducing effects. Interestingly, clinical studies have previously shown that the finding of nonfunctional p53 and high levels of HIF-1α portends a particularly poor prognosis (Birner et al., 2001). The combined HIF-1 blockade/radiotherapy regimen described above may be highly effective for this difficult-to-treat tumor population, suggesting again

that patient selection may be critical to optimizing this therapeutic option. These issues warrant further study.

Experimental procedures

Cloning
For details, please see the Supplemental Data.

Irradiation
Radiation was delivered using a Mark IV cesium irradiator (dose rate = 7 Gy/min; JL Shepherd) to the specified dose. Cells were irradiated in a single fraction. Tumors were irradiated in three fractions, spaced by 12 hr each, to the specified doses.

Caspase assay
Samples of 10^3 cells, plated in 96-well plates, were analyzed for caspase activity 6 hr after irradiation using the Caspase-Glo 3/7 kit (Promega).

DNA content analysis
Cells were harvested 48 hr after treatment, fixed in ice-cold 70% ethanol, and stained with propidium iodide (Sigma) in the presence of RNase (Qiagen). Flow cytometry was then used to determine the relative sizes of the apoptotic, G1, S, and G2/M cell populations.

Protein analysis
For details, please see the Supplemental Data.

Clonogenic assay
Cells were pretreated as indicated, harvested, exposed to the specified doses of radiation, and then sparsely plated. Seven days later, cells were fixed in methanol:acetone and stained with crystal violet to facilitate counting of colonies ($\geq$50 cells). Clonogenic survival was calculated for each radiation dose after correcting for plating efficiency.

Glucose consumption
After 24 hr of the indicated treatment, samples of tissue culture media were analyzed using microdialysis (CMA/Microdialysis). The difference in glucose content in the media between 0 and 24 hr, normalized to protein content in the media, was calculated as the glucose consumption rate.

In vitro ATP assay
After 24 hr of treatment, samples of 10^3 cells in 96-well plates were assayed for total cellular ATP levels using the CellTiter-Glo Luminescent Cell Viability Kit (Promega).

Immunohistochemistry
For details, please see the Supplemental Data.

Ex vivo bioluminescence ATP assay
For details, please see the Supplemental Data.

Window chamber studies
Window chambers were implanted and imaged as previously described (Moeller et al., 2004). Tumors were implanted by injecting 10^4 4T1 cells or 10^5 HCT116 cells into the dorsal skinfold at the time of surgery. Treatments were not initiated for window chamber tumors until they had a vascular network allowing visible blood flow across the entire tumor. ImageJ was used to trace and measure the length of the vasculature in window chamber tumors. Total vascular length was then divided by the two-dimensional tumor area, determined using ImageJ, to calculate the vascular length density.

Growth delay studies
HCT116 cells (10^6) were injected into the flank of athymic nude mice. Tumor volumes were calculated every 3–4 days, based on caliper measurements of the short (a) and long (b) tumor diameters (volume = $a^2b/2$). Animals were randomized to treatment groups once the average tumor volume surpassed 50 mm^3. Animals in each group were sacrificed once the average tumor volume for that group reached 1000 mm^3.

Supplemental data
The Supplemental Data include Supplemental Results, Experimental Procedures, and four figures and can be found with this article online at http://www.cancercell.org/cgi/content/full/8/2/99/DC1/.

Acknowledgments

Support was provided by funds from the Duke SPORE in breast cancer, NIH/NCI CA40355, Aeolus Pharmaceuticals, the Howard Hughes Medical Institute, and the Duke Medical Scientist Training Program. Support provided for M.R.D. by Ashutosh Chilkoti (NIH EB00188-01).

Received: March 30, 2005
Revised: May 27, 2005
Accepted: June 28, 2005
Published: August 15, 2005

References

Abend, M. (2003). Reasons to reconsider the significance of apoptosis for cancer therapy. Int. J. Radiat. Biol. *79*, 927–941.

Aebersold, D.M., Burri, P., Beer, K.T., Laissue, J., Djonov, V., Greiner, R.H., and Semenza, G.L. (2001). Expression of hypoxia-inducible factor-1α: a novel predictive and prognostic parameter in the radiotherapy of oropharyngeal cancer. Cancer Res. *61*, 2911–2916.

Akakura, N., Kobayashi, M., Horiuchi, I., Suzuki, A., Wang, J., Chen, J., Niizeki, H., Kawamura, K., Hosokawa, M., and Asaka, M. (2001). Constitutive expression of hypoxia-inducible factor-1α renders pancreatic cancer cells resistant to apoptosis induced by hypoxia and nutrient deprivation. Cancer Res. *61*, 6548–6554.

An, W.G., Kanekal, M., Simon, M.C., Maltepe, E., Blagosklonny, M.V., and Neckers, L.M. (1998). Stabilization of wild-type p53 by hypoxia-inducible factor 1α. Nature *392*, 405–408.

Berry, R.J., Hall, E.J., and Cavanagh, J. (1970). Radiosensitivity and the oxygen effect for mammalian cells cultured in vitro in stationary phase. Br. J. Radiol. *43*, 81–90.

Birner, P., Schindl, M., Obermair, A., Breitenecker, G., and Oberhuber, G. (2001). Expression of hypoxia-inducible factor 1α in epithelial ovarian tumors: its impact on prognosis and on response to chemotherapy. Clin. Cancer Res. *7*, 1661–1668.

Bos, R., van der Groep, P., Greijer, A.E., Shvarts, A., Meijer, S., Pinedo, H.M., Semenza, G.L., van Diest, P.J., and van der Wall, E. (2003). Levels of hypoxia-inducible factor-1α independently predict prognosis in patients with lymph node negative breast carcinoma. Cancer *97*, 1573–1581.

Camphausen, K., and Tofilon, P.J. (2004). Combining radiation and molecular targeting in cancer therapy. Cancer Biol. Ther. *3*, 247–250.

Carmeliet, P., Dor, Y., Herbert, J.M., Fukumura, D., Brusselmans, K., Dewerchin, M., Neeman, M., Bono, F., Abramovitch, R., Maxwell, P., et al. (1998). Role of HIF-1α in hypoxia-mediated apoptosis, cell proliferation and tumour angiogenesis. Nature *394*, 485–490.

Chandel, N.S., Maltepe, E., Goldwasser, E., Mathieu, C.E., Simon, M.C., and Schumacker, P.T. (1998). Mitochondrial reactive oxygen species trigger hypoxia-induced transcription. Proc. Natl. Acad. Sci. USA *95*, 11715–11720.

Denekamp, J. (1986). Cell kinetics and radiation biology. Int. J. Radiat. Biol. Relat. Stud. Phys. Chem. Med. *49*, 357–380.

Firth, J.D., Ebert, B.L., and Ratcliffe, P.J. (1995). Hypoxic regulation of lactate dehydrogenase A. Interaction between hypoxia-inducible factor 1 and cAMP response elements. J. Biol. Chem. *270*, 21021–21027.

Garcia-Barros, M., Paris, F., Cordon-Cardo, C., Lyden, D., Rafii, S., Haimovitz-Friedman, A., Fuks, Z., and Kolesnick, R. (2003). Tumor response to radiotherapy regulated by endothelial cell apoptosis. Science *300*, 1155–1159.

Giaccia, A., Siim, B.G., and Johnson, R.S. (2003). HIF-1 as a target for drug development. Nat. Rev. Drug Discov. *2*, 803–811.

Goda, N., Ryan, H.E., Khadivi, B., McNulty, W., Rickert, R.C., and Johnson, R.S. (2003). Hypoxia-inducible factor 1α is essential for cell cycle arrest during hypoxia. Mol. Cell. Biol. *23*, 359–369.

Gorski, D.H., Beckett, M.A., Jaskowiak, N.T., Calvin, D.P., Mauceri, H.J., Salloum, R.M., Seetharam, S., Koons, A., Hari, D.M., Kufe, D.W., and Weichselbaum, R.R. (1999). Blockage of the vascular endothelial growth factor stress response increases the antitumor effects of ionizing radiation. Cancer Res. *59*, 3374–3378.

Griffiths, J.R., McSheehy, P.M., Robinson, S.P., Troy, H., Chung, Y.L., Leek, R.D., Williams, K.J., Stratford, I.J., Harris, A.L., and Stubbs, M. (2002). Metabolic changes detected by in vivo magnetic resonance studies of HEPA-1 wild-type tumors and tumors deficient in hypoxia-inducible factor-1β (HIF-1β): evidence of an anabolic role for the HIF-1 pathway. Cancer Res. *62*, 688–695.

Guo, K., Searfoss, G., Krolikowski, D., Pagnoni, M., Franks, C., Clark, K., Yu, K.T., Jaye, M., and Ivashchenko, Y. (2001). Hypoxia induces the expression of the pro-apoptotic gene BNIP3. Cell Death Differ. *8*, 367–376.

Heller, D.P., and Raaphorst, G.P. (1994). Inhibition of potentially lethal damage recovery by altered pH, glucose utilization and proliferation in plateau growth phase human glioma cells. Int. J. Radiat. Biol. *66*, 41–47.

Koukourakis, M.I., Giatromanolaki, A., Sivridis, E., Simopoulos, C., Turley, H., Talks, K., Gatter, K.C., and Harris, A.L. (2002). Hypoxia-inducible factor (HIF1A and HIF2A), angiogenesis, and chemoradiotherapy outcome of squamous cell head-and-neck cancer. Int. J. Radiat. Oncol. Biol. Phys. *53*, 1192–1202.

Kung, A.L., Wang, S., Klco, J.M., Kaelin, W.G., and Livingston, D.M. (2000). Suppression of tumor growth through disruption of hypoxia-inducible transcription. Nat. Med. *6*, 1335–1340.

Laughner, E., Taghavi, P., Chiles, K., Mahon, P.C., and Semenza, G.L. (2001). HER2 (neu) signaling increases the rate of hypoxia-inducible factor 1α (HIF-1α) synthesis: novel mechanism for HIF-1-mediated vascular endothelial growth factor expression. Mol. Cell. Biol. *21*, 3995–4004.

Luk, C.K., and Sutherland, R.M. (1987). Nutrient modification of proliferation and radiation response in EMT6/Ro spheroids. Int. J. Radiat. Oncol. Biol. Phys. *13*, 885–895.

Maxwell, P.H., Dachs, G.U., Gleadle, J.M., Nicholls, L.G., Harris, A.L., Stratford, I.J., Hankinson, O., Pugh, C.W., and Ratcliffe, P.J. (1997). Hypoxia-inducible factor-1 modulates gene expression in solid tumors and influences both angiogenesis and tumor growth. Proc. Natl. Acad. Sci. USA *94*, 8104–8109.

Michel, G., Minet, E., Mottet, D., Remacle, J., and Michiels, C. (2002). Site-directed mutagenesis studies of the hypoxia-inducible factor-1α DNA-binding domain. Biochim. Biophys. Acta *1578*, 73–83.

Moeller, B.J., Cao, Y., Li, C.Y., and Dewhirst, M.W. (2004). Radiation activates HIF-1 to regulate vascular radiosensitivity in tumors: role of reoxygenation, free radicals, and stress granules. Cancer Cell *5*, 429–441.

Murata, R., Nishimura, Y., and Hiraoka, M. (1997). An antiangiogenic agent (TNP-470) inhibited reoxygenation during fractionated radiotherapy of murine mammary carcinoma. Int. J. Radiat. Oncol. Biol. Phys. *37*, 1107–1113.

Ravi, R., Mookerjee, B., Bhujwalla, Z.M., Sutter, C.H., Artemov, D., Zeng, Q., Dillehay, L.E., Madan, A., Semenza, G.L., and Bedi, A. (2000). Regulation of tumor angiogenesis by p53-induced degradation of hypoxia-inducible factor 1α. Genes Dev. *14*, 34–44.

Rojas, A., and Denekamp, J. (1989). Modifiers of radiosensitivity. Experientia *45*, 41–52.

Rupnow, B.A., and Knox, S.J. (1999). The role of radiation-induced apoptosis as a determinant of tumor responses to radiation therapy. Apoptosis *4*, 115–143.

Ryan, H.E., Lo, J., and Johnson, R.S. (1998). HIF-1α is required for solid tumor formation and embryonic vascularization. EMBO J. *17*, 3005–3015.

Schwickert, G., Walenta, S., and Mueller-Klieser, W. (1996). Mapping and quantification of biomolecules in tumor biopsies using bioluminescence. Experientia *52*, 460–463.

Semenza, G.L. (2002). HIF-1 and tumor progression: pathophysiology and therapeutics. Trends Mol. Med. *8*, S62–S67.

Semenza, G.L. (2003). Targeting HIF-1 for cancer therapy. Nat. Rev. Cancer *3*, 721–732.

Semenza, G.L., Roth, P.H., Fang, H.M., and Wang, G.L. (1994). Transcriptional regulation of genes encoding glycolytic enzymes by hypoxia-inducible factor 1. J. Biol. Chem. *269*, 23757–23763.

Shibaji, T., Nagao, M., Ikeda, N., Kanehiro, H., Hisanaga, M., Ko, S., Fukumoto, A., and Nakajima, Y. (2003). Prognostic significance of HIF-1α overexpression in human pancreatic cancer. Anticancer Res. *23*, 4721–4727.

Sowter, H.M., Ratcliffe, P.J., Watson, P., Greenberg, A.H., and Harris, A.L. (2001). HIF-1-dependent regulation of hypoxic induction of the cell death factors BNIP3 and NIX in human tumors. Cancer Res. *61*, 6669–6673.

Stoeltzing, O., McCarty, M.F., Wey, J.S., Fan, F., Liu, W., Belcheva, A., Bucana, C.D., Semenza, G.L., and Ellis, L.M. (2004). Role of hypoxia-inducible factor 1α in gastric cancer cell growth, angiogenesis, and vessel maturation. J. Natl. Cancer Inst. *96*, 946–956.

Tang, N., Wang, L., Esko, J., Giordano, F.J., Huang, Y., Gerber, H.P., Ferrara, N., and Johnson, R.S. (2004). Loss of HIF-1α in endothelial cells disrupts a hypoxia-driven VEGF autocrine loop necessary for tumorigenesis. Cancer Cell *6*, 485–495.

Wang, G.L., and Semenza, G.L. (1993). General involvement of hypoxia-inducible factor 1 in transcriptional response to hypoxia. Proc. Natl. Acad. Sci. USA *90*, 4304–4308.

Winkler, F., Kozin, S.V., Tong, R.T., Chae, S.S., Booth, M.F., Garkavtsev, I., Xu, L., Hicklin, D.J., Fukumura, D., di Tomaso, E., et al. (2004). Kinetics of vascular normalization by VEGFR2 blockade governs brain tumor response to radiation: role of oxygenation, angiopoietin-1, and matrix metalloproteinases. Cancer Cell *6*, 553–563.

Zhong, H., De Marzo, A.M., Laughner, E., Lim, M., Hilton, D.A., Zagzag, D., Buechler, P., Isaacs, W.B., Semenza, G.L., and Simons, J.W. (1999). Overexpression of hypoxia-inducible factor 1α in common human cancers and their metastases. Cancer Res. *59*, 5830–5835.

Zundel, W., Schindler, C., Haas-Kogan, D., Koong, A., Kaper, F., Chen, E., Gottschalk, A.R., Ryan, H.E., Johnson, R.S., Jefferson, A.B., et al. (2000). Loss of PTEN facilitates HIF-1-mediated gene expression. Genes Dev. *14*, 391–396.